

Flame-retardancy and photocatalytic properties of cellulosic fabric coated by nano-sized titanium dioxide

Hadi Fallah Moafi · Abdollah Fallah Shojaie ·
Mohammad Ali Zanjanchi

Received: 24 December 2009 / Accepted: 26 October 2010 / Published online: 24 December 2010
© Akadémiai Kiadó, Budapest, Hungary 2010

Abstract We have investigated the effect of titanium dioxide as a durable finish on the flammability and photocatalytic self-cleaning of cellulosic fabric. Nano-sized titanium dioxide particles were successfully synthesized and deposited onto cellulosic fibers with good compatibility, significant photocatalytic self-cleaning activity, and flame-retardancy properties using the sol–gel process at low temperature. The photocatalytic activity was tested by measuring the photodegradation of methylene blue under ultraviolet–visible illumination, and also flame-retardancy effect was tested by flammability tester. The samples have been characterized by several techniques such as scanning electron microscopy, transmission electron microscopy, diffuse reflectance spectroscopy, X-ray diffraction, and thermogravimetric analysis. The titanium dioxide nanoparticles with 10–20 nm in size have been found to form a homogeneous thin film on the fiber surface which shows efficient photocatalytic and flame-retardancy properties. This preparation technique can also be applied to new fabrics to create self-cleaning and flame-retardancy properties in them.

Keywords Cellulosic fabric · Flame-retardancy · Sol–gel · Self-cleaning · Titanium dioxide · Thermal analysis

Introduction

The field of flame-retardancy of polymers has greatly developed and expanded during the last 20 years [1]. Most

polymers and cellulosic fibers as organic materials are very sensitive to flame. Therefore, the improvement of their flame-retardancy has become more and more important to comply with the safety requirements. A flame-retardant is a compound or mixture of components that, when added or incorporated chemically and or physically into a polymer, serves to hinder the ignition or growth of fire.

The progression of perpetual self-cleaning textiles is an objective sought by the textile industry in the framework of new products classified as intelligent textiles [2, 3].

Self-cleaning applications using semiconducting powders or thin films have become a subject of increasing interest especially in the last 20 years. Among semiconductor oxides, TiO_2 is one of the most widely used materials for self-cleaning application [4–9].

Nano-sized anatase TiO_2 has been widely used as an efficient photocatalyst for the photodegradation of organic pollutants in various phases owing to its thermostability, inexpensiveness, non-toxicity, strong oxidizing power, and long-term photostability [10–13].

The direct preparation of anatase/polymer nanocomposite films from sol–gel titania on polymer films is generally not possible due to the low resistance of the organic polymers to heat treatment [14].

Recently, several studies on the formation processes of anatase nanoparticles, onto different polymers including cellulose surface at relatively low temperatures, have been published [15–26]. Among these, the following processes can be highlighted to obtain: (a) self-cleaning of cotton textiles modified with TiO_2 at low temperatures under daylight irradiation [19], (b) anatase nanocrystals deposited on cotton fabrics from titanium isopropoxide (TIP) solutions by sol–gel process [23], (c) synthesis and characterization of self-cleaning cotton fabrics modified by TiO_2 through a facile approach [25], (d) self-cleaning modified

H. F. Moafi · A. F. Shojaie (✉) · M. A. Zanjanchi
Department of Chemistry, Faculty of Science,
University of Guilan, P.O. Box 1914, Rasht, Iran
e-mail: a.f.shojaie@guilan.ac.ir

TiO₂-cotton pretreated by UVC-light and RF-plasma in vacuum and also under atmospheric pressure [26].

The aim of this investigation is to study the effect of deposited titanium dioxide as a flame-retardant for the impartation of flame-retardancy and also as a semiconducting photocatalyst for self-cleaning properties to create photoactive flame-retarded cellulosic fabric. This innovation is important because it should allow its practical use for industrial applications.

Experimental

Materials

Pure cellulosic fiber characterized by 10 μm diameter from cotton was used for the entire process. Methylene blue (MB) of AR grade obtained from Merck (Germany) was used for the experiments. Other chemicals were obtained from Merck (Germany) and used as such without further purification. Water used in our experiments was triply distilled.

Synthesis procedure (preparation of TiO₂ nanosol)

The typical procedure for synthesis of nano TiO₂ onto cellulosic fibers is as follows.

Titanium (IV) isopropoxide (TIP) was used as a precursor of TiO₂. A solution was prepared as follows: Titanium (IV) isopropoxide (0.02 mol) was added to 2-isopropanol under vigorous stirring conditions and then triethylamine (0.005 mol) was added as a stabilizer of the solution and stirred (200 rpm) for 15 min. Another solution was then prepared separately as follows: hydrochloric acid (1 mL) and water (0.5 mL) were added to 2-isopropanol and mixed well by a magnetic stirrer for 10 min. This solution (50 mL) was then added dropwise into above mixture (50 mL) consisting of titanium (IV) isopropoxide (TIP), isopropanol, and triethylamine, and stirred vigorously at room temperature to

carry out hydrolysis. Subsequently, after continuous stirring for 2 h, the yellowish transparent sol was obtained (100 mL). The formed TiO₂ sol was transparent and quite stable.

For the impregnation, fabric samples (2 cm × 2 cm) were treated with hot distilled water and acetone for 60 min to remove impurities and dried at room temperature for 24 h. The cellulosic fabric after dried in a preheated oven is then immersed for 5 min in the TiO₂ containing liquid nanosol. The extracted samples were then squeeze rolled and placed in 70 °C preheated oven to remove the solvent from the fiber and then heated at 110 °C for 30 min, to complete the formation of titanium dioxide from the precursor. Finally, the impregnated fibers were rinsed in distilled water. During this step, the unattached TiO₂ particles were removed from the fiber surface.

Flame-retardancy experiment

All cellulosic fabrics were a plain construction, weighing 144 g m⁻², unfinished 100% cotton, laundered, and dried. They were 22 × 8 cm strips cut along the warp direction and pre-washed in hot distilled water. The specimens were dried at 110 °C for 30 min in an oven, cooled in a desiccator, and weighed with an analytical precision.

With the exception of the first set (Table 1), all other specimens were impregnated with above as-prepared TiO₂ nanosol at 20 °C. Afterward, they were squeeze rolled and dried horizontally in an oven at 110 °C for 30 min. They were then cooled in a desiccator and re-weighed with an analytical balance so that the suitable add-on presented onto the samples was obtained.

Flammability test

A vertical test method for the estimation of the fabric's combustibility has been designed and named as Mostashari's flammability tester. The conditions of the fabrics and environment were on an average temperature ranged

Table 1 The effect of deposited titanium dioxide on the flame-retardancy imparted to cellulosic fabric

Set no. ^a	Samples	Percent (add-on) drying at 110 °C and weighing	Burning time/s	Burning rate/cm s ⁻¹	Char length/cm	State of the fabric
1	Untreated	–	25	0.88	–	CB
2	Treated ^b	4.80	–	–	1	FR
3	Treated ^c	7.44	–	–	0.5	FR

CB completely burnt, FR flame-retarded

^a Average of five tests for each set

^b Treated sample with nanosol after washing

^c Treated sample with nanosol before washing

Notes: (1) For flame-retardancy (FRs) samples, the char length ≤2.0 cm, (2) percent (add-on) means the mass of addition for impregnated dry fabrics × 100

between 20 and 22 °C and relative humidity (RH) ranged between 65 and 67%. The similar procedure is described in DOC FF 3-71 [27]. The full description of our flammability tester has been demonstrated in the previous investigations [28–38].

Photocatalytic test

The photoactivity of the titanium dioxide-coated cellulosic fibers has been investigated by exposing the samples containing adsorbed MB to UV–Vis light.

For this purpose, 100 mL aqueous solutions ($1.0 \times 10^{-5} \text{ mol L}^{-1}$) of MB were prepared. Both bare and TiO₂-covered fibers are treated in MB solution. The same amount of each sample was immersed under mild stirring in the same amount of the solution and remained overnight to complete the adsorption. The solution was then removed and the samples dried at room temperature. The so-obtained samples were then exposed to UV–Vis to test their photoactivity. For photocatalytic reactions, the irradiation was carried out on dry samples, by means of a high-pressure mercury lamp (HPMV 400 W, Germany). The lamp yields a spectrum ranging from ultraviolet to visible (200–800 nm). The distance between the lamp and reactor was 50 cm, and the intensity of the UV radiation reaching the reactor was measured to be about 20 mW cm^{-2} by a radiometer.

The photocatalytic decomposition rate was determined from the following equation.

$$\text{Photocatalytic decomposition} = (C_0 - C)/C_0 \\ = (A_0 - A)/A_0$$

where C_0 represents the initial concentration of the dyes on fiber surface, C the final concentration after illumination by

UV light, A_0 the initial absorbance, and A the variable absorbance.

Characterization techniques

To investigate the morphology of the pure and TiO₂-modified cellulosic fibers, scanning electron microscopy (SEM) images were obtained on a Philips, XL30 equipped with energy dispersive (EDS) microanalysis system for compositional analysis of the TiO₂-coated cellulosic fibers. The TiO₂ particle sizes were obtained by transmission electron microscope (TEM) images on a Philips CM10 instrument with an accelerating voltage of 100 kV. For photodecomposition reaction, the UV–Vis reflectance spectra were recorded at room temperature by a UV-2100 Shimadzu Spectrophotometer in the reflectance mode by investigating the evolution of the absorbance.

X-ray diffraction measurements were recorded by a D8 Bruker advance diffractometer with Cu K_α radiation, scan rate $0.02 \text{ } 2\theta/\text{s}$ and within a range of 2θ of 10–70 at room temperature.

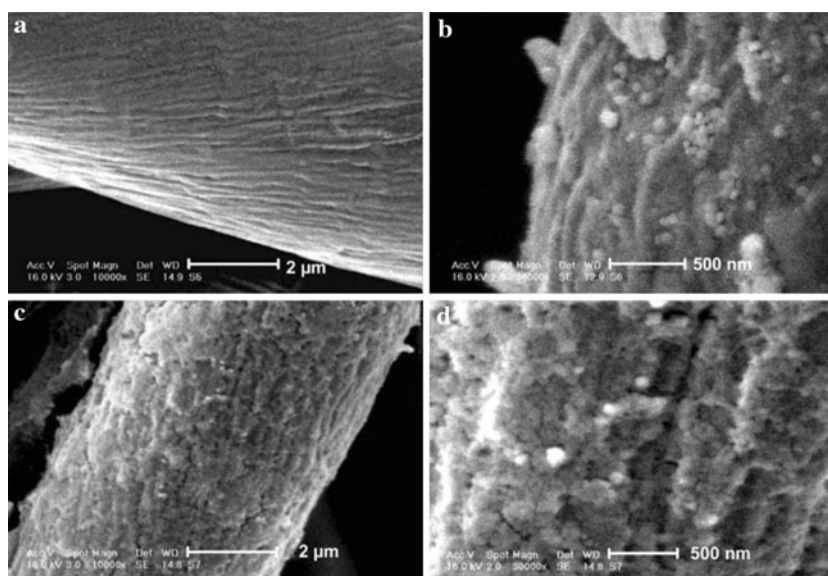
To investigate the thermal behavior of samples, thermogravimetric analysis was performed under air and nitrogen atmosphere at a heating rate of $10 \text{ } ^\circ\text{C min}^{-1}$ using a thermogravimetric analyzer (TGA V5.1A DuPont 2000).

Results and discussion

SEM, TEM images, and EDS analysis of TiO₂ coatings

In order to investigate the morphology of the obtained samples, comparison between the SEM images of the treated and untreated cellulosic fibers is illustrated in

Fig. 1 SEM images of **a** pure fiber ($\times 10,000$), **b** TiO₂-coated fiber after washing ($\times 30,000$), **c** TiO₂-coated fiber before washing ($\times 10,000$), and **d** TiO₂-coated fiber before washing ($\times 30,000$)



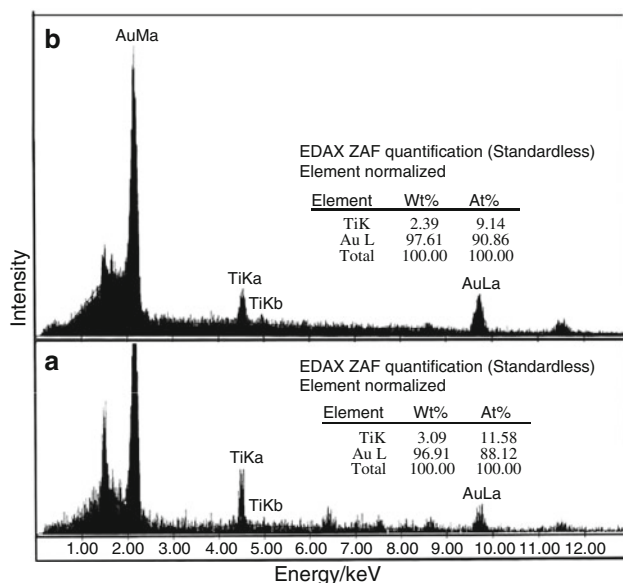


Fig. 2 EDS spectra of TiO₂-coated cellulose fibers **a** before washing and **b** after washing

Fig. 1. It clearly shows that treated fiber before and after washing is covered by a continuous and homogeneous TiO₂ thin film. SEM study of TiO₂ thin film deposited onto cellulose fibers indicate that the particle size of the deposited titania on the fibers surface is less than 100 nm (Fig. 1d, b).

In Fig. 2, the EDS analysis of TiO₂-covered fibers before washing (a) and after washing (b) is reported. On the basis of this result, it is noteworthy to observe that the deposited material consists of titanium and oxygen and after washing, remarkable amount of titania is still present on the cellulose fibers surface. This means that TiO₂ particles are firmly anchored to the surface of fibers.

In order to investigate the size of TiO₂ particles forming the TiO₂ film, a portion of the material was collected by scratching the surface and was analyzed by TEM. TEM images, reported in Fig. 3, show that the deposited titania film consists of spherical particles of average diameter 10–20 nm (Fig. 3a, b).

X-ray diffraction (XRD) analysis

The XRD patterns of pure, titania-coated cellulose fibers and sol-gel derived TiO₂ powders are reported in Fig. 4. Figure 4a reports two broad peaks and one intense peak at 13.16°, 15.12°, and 21.4°, respectively, which comprise the typical XRD pattern of cellulose fibers [39]. Two of three major peaks at 13.16° and 15.12° are related to amorphous phase of fiber, while the peak at 21.4° is due to the crystalline phase.

Figure 4b shows XRD pattern of TiO₂-covered fibers. Since the amount of TiO₂ onto surface fibers was low,

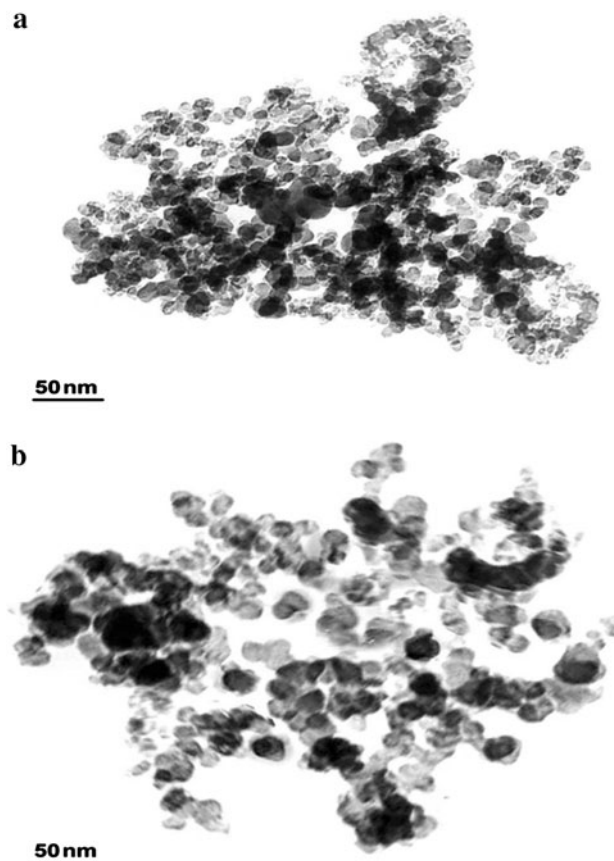


Fig. 3 TEM images of **a** TiO₂ nanoparticles forming the TiO₂ film and **b** magnified TEM image of TiO₂ nanoparticles

therefore TiO₂ on the fibers surface did not show good crystalline phase intensity in XRD pattern. However, small peaks were observed at $2\theta = 25^\circ, 37^\circ,$ and 48° . These are associated with diffraction peaks corresponding to anatase crystallites.

Figure 4c and d shows XRD patterns of sol-gel-derived TiO₂ powders calcined at 500 and 700 °C, respectively.

TiO₂ powder calcined at 500 °C in the spectrum of TiO₂ is easily identified as the crystal of anatase form, whereas at 700 °C is easily taken as the crystal of rutile form.

Flame-retardancy analysis

The experimental results of analysis are summarized to identify the burning characteristics of the specimens in Table 1. Vertical flame spread tests were carefully conducted to determine the add-on values on the burning time in seconds in column 3. The states of the specimens (after the tests) are illustrated in column 7, CB means complete burn, and FR stands for flame-retardation. The burning rates in cm s⁻¹ were calculated by means of dividing the length of the burned fabrics by their burning time shown in column 5. Char lengths in cm are given in column 6. It can

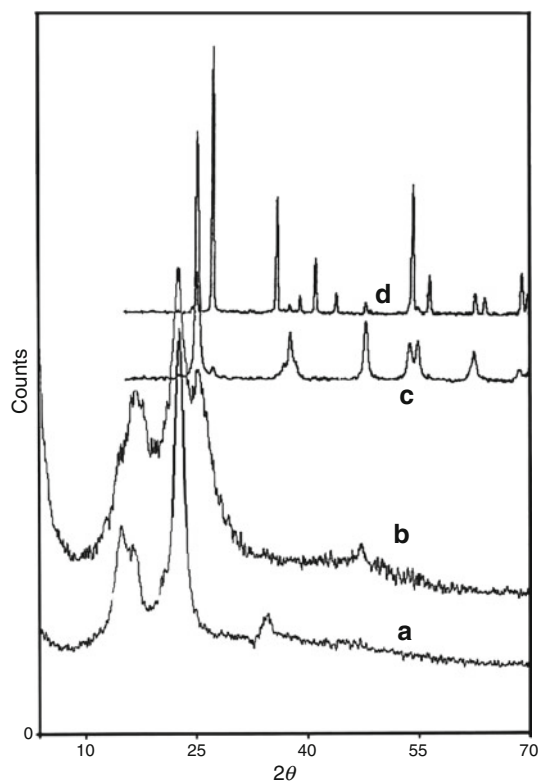


Fig. 4 XRD patterns of samples: (a) pure cellulosic fibers, (b) TiO₂-covered fibers, (c) sol-gel-derived TiO₂ powder at 500 °C (d) sol-gel-derived TiO₂ powder at 800 °C

be deduced from the experimental results of column 3 that the efficient quantity of titanium oxide as a flame-retardant to cellulosic fabric expressed in g per 100 g of dried fabric is about 4.8%. Moreover, this add-on value is an efficient amount for impartation of flame-retardancy to the cellulosic fabric.

Concerning thermogravimetry (TG), it is widely used to investigate the thermal decomposition of polymers to assess their relative thermal stabilities and the pathway of combustion and pyrolysis. TG curves of the samples under nitrogen and air atmospheres are given in Fig. 5. TG curve of untreated cellulosic fibers (Fig. 5a) reveals that its pyrolysis includes three stages: initial, main, and char decomposition steps [40]. The related temperature, speed, and mass loss of every stage can be found from the TG curve.

In the initial stage, where the temperature range is below 300 °C, the most important changes of the polymer occur in its physical properties and little mass loss happens. Here, the damage to cellulose occurs mostly in its amorphous region. The main pyrolysis stage occurs in the temperature range of 300–370 °C. In this stage, the mass loss is very fast and significant. Most of pyrolysis products are produced in this stage. Referring to the literature, glucose is one of the major products, together with all kinds of combustible gases [40].

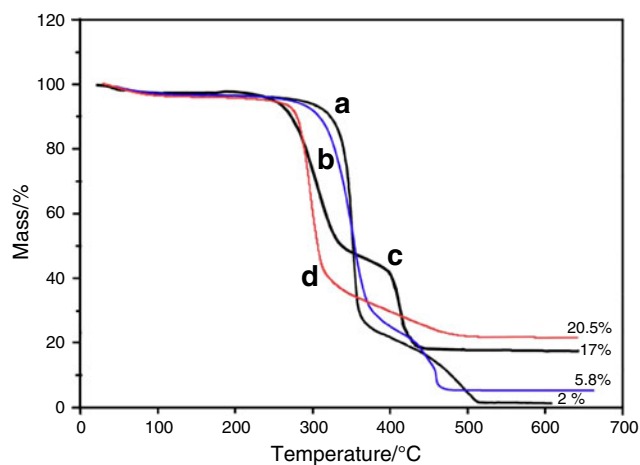


Fig. 5 TG comparative curves of untreated and treated cellulosic fabric with TiO₂ to impart flame-retardancy: (a) untreated fabric under air atmosphere, (b) untreated fabric under nitrogen atmosphere, (c) treated cellulosic fabric with TiO₂ under air atmosphere, and (d) treated cellulosic fabric with TiO₂ under nitrogen atmosphere

The char pyrolysis occurs at the temperature above 370 °C. During this process, dehydration and charring reactions complete with the production of glucose, with the dehydration and charring reactions being more obvious. The mass decomposition continues to dehydration and decarboxylation, releasing more water and carbon dioxide, and producing double bond and carbonyl products. The carbon content in the decomposed products becomes higher and higher, and charred residues are formed. Although the exact temperature ranges of cellulose pyrolysis may vary depending on different cellulosic materials and experimental conditions, the three steps always exist in pyrolysis of cellulose. In fact, the pyrolysis will go from amorphous regions to crystalline regions in cellulose [40].

The outcomes of TG curves concerning the flame-retarded supported samples show the similar three stages but with lower decomposition temperatures and mass loss, i.e., these stages happen well below under the thermal degradation of untreated cellulose. It is obvious that the decomposition temperature of the treated substrate with TiO₂ is lower than the untreated one (Fig. 5c, d), that indicating the influence of TiO₂ as a flame-retardant agent. Untreated fiber started rapid thermal degradation at 300 °C and lost about 98% of this mass at 550 °C (Fig. 5a). However, the treated sample at the optimum level of addition for impartation of flame-retardancy started degradation ranging from 250 °C. It is mentionable that the major mass loss for untreated fiber occurred at 350 °C about 70% of its mass was lost. However, the treated sample lost only 50% of its mass at this temperature. Therefore, it can be deduced that by the application of titanium dioxide as a flame-retardant, the formation of

volatile pyrolysis products has been postponed when the polymer is subjected to the thermal degradation.

TG curve samples under nitrogen atmospheres show the similar three stages (Fig. 5b). The untreated cotton fabric (curve b) has a decomposition temperature starting at 300 °C where the treated fabrics have lower decomposition temperatures because of a catalytic dehydration of cellulose by the flame-retardant (Fig. 5d).

It can be observed that a noticeable reduction have occurred at the initiating stage of treated sample that this could be due to the catalytic effect of TiO₂ nanoparticles and interaction of functional groups of cellulose fiber and hydroxyl groups on the surface of fiber with nanoparticles.

However, the remaining residue, i.e., TiO₂, seems to play the role of dust or wall for heat absorption and dissipation in the combustion zone as described in the Wall Effect Theory [41]. According to this theory, “if a high enough concentration of dust is present in the air, no flame can propagate.” Hence a lowering of temperature is the result and the goal of flame-retardancy could be achieved.

After combustion of all organic part in TiO₂-covered fibers, the residual amount (~17% by mass) corresponds to TiO₂ (Fig. 5c). From this result, it is evident that the thermogravimetric analysis technique in air allows to evaluate the present of TiO₂ covering the cellulosic fibers.

Photocatalytic self-cleaning

The photoactivity of the synthesized titanium dioxide on cellulosic fibers has been investigated by exposing the samples containing adsorbed MB to UV-Vis light. The UV-Vis reflectance spectra obtained on the dried samples before (spectrum a) and after illumination (spectrum b–e)

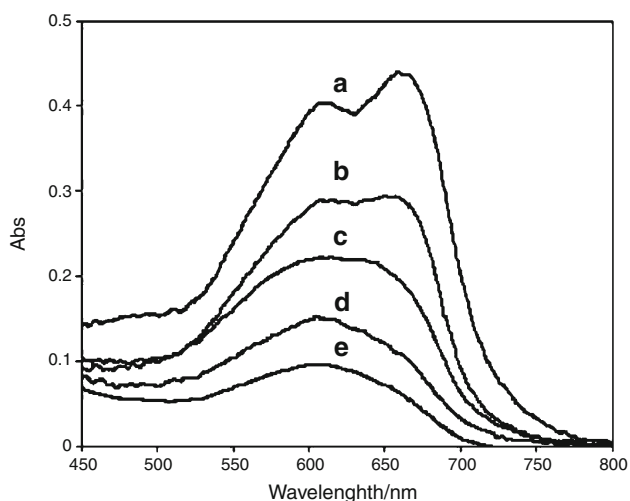


Fig. 6 UV-Vis reflectance spectral changes of MB on TiO₂-coated fibers at room temperature, under UV-Vis light irradiation: spectra a–f for 0, 1, 2, 4, 6, and 8 h irradiation time, respectively

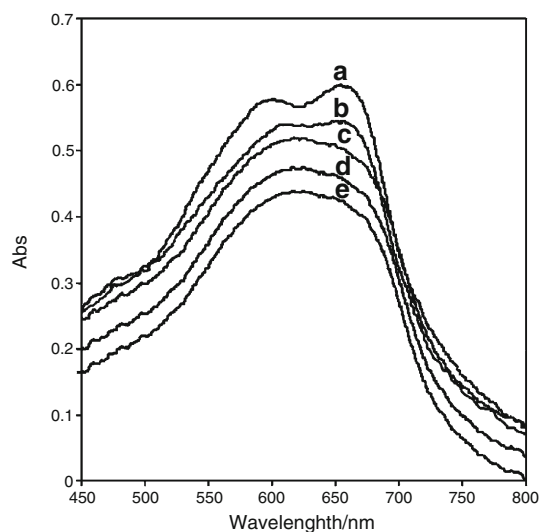


Fig. 7 UV-Vis reflectance spectral changes of MB on pure cellulosic fibers at room temperature, under UV-Vis light irradiation: spectra a–f for 0, 1, 2, 4, 6, and 8 h irradiation time, respectively

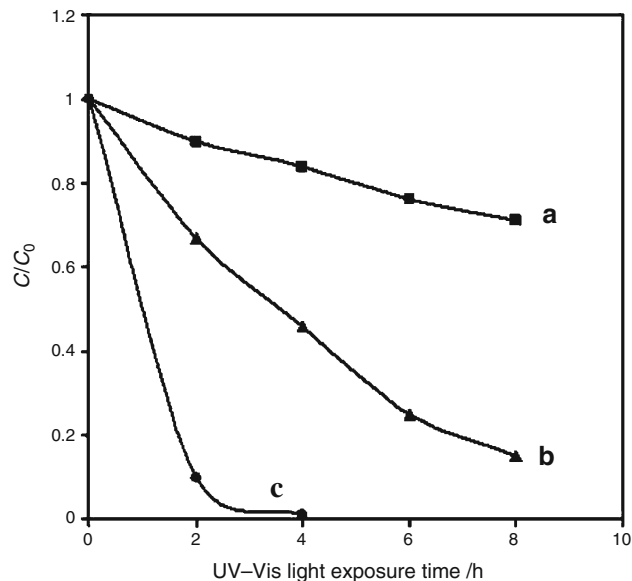


Fig. 8 Time dependence of the surface concentration of adsorbed MB upon light exposure: (a) untreated fibers, (b) photocatalytic activity of TiO₂-coated fibers, and (c) P25 (Degussa), where C₀ is the initial concentration of the dye on surface fiber and C is the final concentration after illumination by UV-Vis light

are reported in Figs. 6 and 7, respectively. From Fig. 6a, it can be observed that the absorption bands in the 500–700 nm interval due to adsorption of MB change rapidly because supported TiO₂ promotes the catalytic photodegradation (spectrum b–f). This is not unexpected since the photocatalytic activity of TiO₂ is well known [42, 43]. The disappearance rate of the band due to MB adsorbed on the TiO₂-covered fibers is much higher than that observed in case of untreated fibers (Fig. 7). Of course,

the photodegradation effect is lower than that observed on P25 (Fig. 8), which is the best TiO₂ catalyst.

It is evident that TiO₂-covered fibers promote the photodegradation process, and the high-surface area associated with the small particle size ensures a favorable condition for a relatively fast degradation.

Conclusions

Nano-sized TiO₂-coated cellulosic fibers were successfully prepared by sol–gel technique at low temperature with significant photocatalytic self-cleaning and flame-retardancy activity. This preparation allows to deposit and to graft TiO₂ nanoparticles on fibers, and titanium dioxide covers uniformly surface of the fibers. The TiO₂-covered cellulosic fibers show high-photocatalytic efficiency in decomposing the pre-adsorbed MB under UV–Vis light. Supported TiO₂ particles on cellulosic textiles promote the photodegradation process and fire-retardancy. The high surface area associated with the small particle size ensures a favorable condition for self-cleaning purposes. Flame-retardancy action of the remained TiO₂ in the consumed ashes could be referred due to Dust or Wall Effect Theory suggested by Jolles. That is, the enough concentration of the dust in the flame zone absorbs the heat and causes the heat dissipation. Hence leading to lowering of temperature and consequently to retardation of the flame.

Acknowledgements The authors are grateful to the University of Guilan for financial assistance of this research project.

References

- Lewin M. Unsolved problems and unanswered questions in flame retardance of polymers. *Polym Degrad Stab.* 2005;88:13–9.
- Fujishima A, Hashimoto K, Watanabe T. *Photocatalysis, fundamental and applications.* Tokyo: BKC Inc; 1999.
- Mills A, Lee SK. A web-based overview of semiconductor photochemistry-based current commercial applications. *J Photochem Photobiol A.* 2002;152:233–49.
- Cui H, Shen HS, Gao YM, Dwight K, Wold A. Photocatalytic properties of titanium(IV) oxide thin films prepared by spin coating and spray pyrolysis. *Mater Res Bull.* 1993;28:195–201.
- Gao M, Shen HS, Dwight K, Wold A. Preparation and photocatalytic properties of titanium(IV) oxide films. *Mater Res Bull.* 1992;27:1023–30.
- Watanabe T, Nakajima A, Wang R, Minabe M, Koizumi S, Fujishima A. Photocatalytic activity and photoinduced hydrophilicity of titanium dioxide coated glass. *Thin Solid Films.* 1999;351:260–3.
- Ao CH, Lee SC. Indoor air purification by photocatalyst TiO₂ immobilized on activated carbon filter an installed in an air cleaner. *Chem Eng Sci.* 2005;60:103–9.
- Nonami T, Hase H, Funakoshi K. Apatite-coated titanium dioxide photocatalyst for air purification. *Catal Today.* 2004;96:113–8.
- Parra S, Elena SS, Guasaquillo I, Ravindranathan TK. Photocatalytic degradation of atrazine using suspended and supported TiO₂. *Appl Catal B Environ.* 2004;51:107–16.
- Chen XB, Mao SS. Titanium dioxide nanomaterials: synthesis, properties, modifications, and applications. *Chem Rev.* 2007;107:2891–959.
- Li PG, Khor JN, Brucato A. Modeling of an annular photocatalytic reactor for water purification: oxidation of pesticides. *Environ Sci Technol.* 2004;38:3737–45.
- Kamat PV, Huehn R, Nicolaescu RA. “Sense and Shoot” approach for photocatalytic degradation of organic contaminants in water. *J Phys Chem B.* 2002;106:788–94.
- Litter MI. Heterogeneous photocatalysis: transition metal ions in photocatalytic systems. *Appl Catal B Environ.* 1999;23:89–114.
- Dhananjeyan M, Mielczarski E, Thampi K, Buffat P, Bensimon M, Kulik A, Mielczarski J, Kiwi J. Photodynamics and surface characterization of TiO₂ and Fe₂O₃ photocatalysts immobilized on modified polyethylene films. *J Phys Chem B.* 2001;105:12046–55.
- Daoud WA, Xin JH, Zhang YH. Surface functionalization of cellulose fibers with titanium dioxide nanoparticles and their combined bactericidal activities. *Surf Sci.* 2005;599:69–75.
- Daoud WA, Xin JH. Low temperature sol–gel processed photocatalytic titania coating. *J Sol-Gel Sci Technol.* 2004;29:25–9.
- Daoud WA, Xin JH. Synthesis of single-phase anatase nanocrystallites at near room temperatures. *Chem Commun.* 2005;16:2110–2.
- Bozzi A, Yuranova T, Kiwi J. Self-cleaning of wool-polyamide and polyester textiles by TiO₂-rutile modification under daylight irradiation at ambient temperature. *J Photochem Photobiol A.* 2005;172:27–34.
- Bozzi A, Yuranova T, Kiwi J. Self-cleaning of cotton textiles modified with TiO₂ at low temperatures under daylight irradiation. *J Photochem Photobiol A.* 2005;174:156–64.
- Meilert KT, Laub D, Kiwi J. Photocatalytic self-cleaning of modified cotton textiles by TiO₂ clusters attached by chemical spacers. *J Mol Catal A.* 2005;237:101–3.
- Yuranova T, Mosteo R, Bandara J, Laub D, Kiwi J. Self-cleaning cotton textiles surfaces modified by photoactive SiO₂/TiO₂ coating. *J Mol Catal A.* 2006;224:160–7.
- Qi K, Daoud WA, Xin JH, Mak CL, Tang WS, Cheung WP. Self-cleaning cotton. *J Mater Chem.* 2006;16:4567–74.
- Daoud WA, Xin JH. Nucleation and growth of anatase crystallites on cotton fabrics at low temperature. *J Am Ceram Soc.* 2004;87:953–5.
- Daoud WA, Xin JH, Zhang YH, Qi KH. Surface characterization of thin titania films prepared at low temperatures. *J Non-Cryst Solids.* 2005;351:1486–90.
- Wu D, Long M, Zhou J, Cai W, Zhu X, Chen C, Wu Y. Synthesis and characterization of self-cleaning cotton fabrics modified by TiO₂ through a facile approach. *Surf Coat Technol.* 2009;203:3728–33.
- Mejia MI, Marin JM, Restrepo G, Pulgarin C, Mielczarski E, Mielczarski J, Arroyo Y, Lavanchy JC, Kiwi J. Self-cleaning modified TiO₂-cotton pretreated by UVC-light (185 nm) and RF-plasma in vacuum and also under atmospheric pressure. *Appl Catal B.* 2009;91:481–8.
- U.S. Department of Commerce Standard for Flammability of Children’s Sleepwear (DOC.FF 3-71), Federal Register 36, No. 146, July 19; 1971.
- Mostashari SM, Moafi HF. Thermal decomposition pathway of a cellulosic fabric impregnated by magnesium chloride hexahydrate as a flame-retardant. *J Therm Anal Calorim.* 2008;93:589–94.
- Mostashari SM, Moafi HF, Mostashari SZ. TG comparison between the efficiency of deposited ammonium bromide and

- ammonium chloride on the flame-retardancy imparted to cotton fabric. *J Therm Anal Calorim.* 2009;96:535–40.
30. Mostashari SM, Mostashari SZ. Combustion pathway of cotton fabrics treated by ammonium sulfate as a flame-retardant studied by TG. *J Therm Anal Calorim.* 2008;91:437–41.
 31. Mostashari SM, Kamali Nia Y. Detection of copper(II) sulfate's uniformity and its thermal behavior in flammability of cotton fabric spectrophotometric and TG analysis. *J Therm Anal Calorim.* 2008;92:489–93.
 32. Mostashari SM, Fayyaz F. TG of a cotton fabric impregnated by sodium borate decahydrate ($\text{Na}_2\text{B}_4\text{O}_7 \cdot 10\text{H}_2\text{O}$) as a flame-retardant. *J Therm Anal Calorim.* 2008;93:933–6.
 33. Mostashari SM, Mostashari SZ. Thermogravimetric analysis of a cotton fabric incorporated by 'Graham's salt' applied as a flame-retardant. *J Therm Anal Calorim.* 2009;95:187–92.
 34. Mostashari SM, Kamali Nia Y, Fayyaz F. Thermogravimetry of deposited caustic soda used as a flame-retardant for cotton fabric. *J Therm Anal Calorim.* 2008;91:237–41.
 35. Mostashari SM, Baie S. Thermogravimetry studies of cotton fabric's flame-retardancy by means of synergism of lithium bromide and antimony trioxide. *J Therm Anal Calorim.* 2008;94:97–101.
 36. Mostashari SM, Fayyaz F. XRD characterization of the ashes from a burned cellulosic fabric impregnated with magnesium bromide hexahydrate as flame-retardant. *J Therm Anal Calorim.* 2008;92:845–9.
 37. Mostashari SM, Moafi HF. Flame-retardancy of a cellulosic fabric by the application of synergistic effect between ammonium bromide and antimony (III) oxide. *Chin J Chem.* 2009;27:1–10.
 38. Mostashari SM, Kamali Nia Y, Moafi HF. Comparison between the selected hydroxides of groups IA and IIA as flame retardants for cotton fabrics. *Combust Explos Shock.* 2007;43:194–7.
 39. Moharram MA, Nasr TZAE, Hakeem NA. X-ray diffraction and infrared studies on the effect of thermal treatments on cotton celluloses. *J Polym Sci Polym Lett Ed.* 1981;19:183–7.
 40. Zhu P, Sui S, Wang B, Sun K, Sun G. A study of pyrolysis and pyrolysis products of flame-retardant cotton fabrics by DSC, TGA, and PY–GC–MS. *J Anal Appl Pyrolysis.* 2004;71:645–55.
 41. Jolles ZE, Jolles GI. Some notes on flame-retardant mechanisms in polymers. *Plast Polym.* 1972;40:319.
 42. Sandola F, Balzani V. Preparation and characterization of semi conductors. In: Serpone N, Pelizzetti E, editors. *Photocatalysis—fundamentals and applications.* New York: John Wiley & Sons; 1989. p. 9–44.
 43. Kutsuna S, Toma M, Takeuchi K, Ibusuki T. Photocatalytic degradation of some methyl perfluoroalkyl ethers on TiO_2 particles in air: the dependence on the dark-adsorption, the products, and the implication for a possible tropospheric sink. *Environ Sci Technol.* 1999;33:1071–6.